Applied Mechanics and Materials
ISSN: 1662-7482, Vol. 819, pp 250-256
doi:10.4028/www.scientific.net/AMM.819.250

Submitted: 2014-08-30
Revised: 2015-01-25
Accepted: 2015-01-25
Online: 2016-01-06

Impact of Adjacent Building on Outdoor Ventilation around a Layout of Two Buildings

Ayo Samuel Adinoyi[1,a,*], Normah Mohd-Ghazali[1,b], Shuhaimi Mansor[1,c]

[1]Faculty of Mechanical Engineering, Universiti Teknologi Malaysia, 81310 Johor Bahru, Johor, Malaysia

[a]sa_ayo@yahoo.com, [b]normah@fkm.utm.my, [c]shuhaimi@fkm.utm.my

*Corresponding author

Keywords: separation distance, wind velocity ratio, Computational Fluid Dynamics, outdoor air ventilation, buildings height ratio, air exchange rate

Abstract. The outdoor air ventilation impact of a taller building in different configurations of a layout of two adjacent buildings is presented in this paper. The critical parameters investigated are the separation distance (S) between the buildings and the ratio of height of downwind building to that of the building upwind, herein referred to as building height ratio (HR). The aim is to explore intermediate spacing distances which may engender acceptable ventilation around the buildings. A three-dimensional (3-D) numerical simulation employing the Computational Fluid Dynamics technique which adopts the Reynolds-Averaged Navier-Stokes equation and the realizable k-ε turbulence model was used to study the turbulent flow field around the full-scale two-building configurations. Results show that velocity ratio generally increases with height ratio, indicating that more air motion is induced at the pedestrian level as the height of the downwind building increases. For each of the height ratios, there is a spacing distance at which the velocity ratio is highest. The spacing distances at which the maximum velocity ratio occurs for the various height ratios are proposed. The dimensionless air exchange rate generally increases with height ratio, indicating that greater quantity of air from within the cavity between the buildings is exchanged with air from outside the cavity, which should result in better air quality. The findings of the study demonstrate the importance of incorporating wind data of an urban area in formulating guidelines for layout of buildings.

Introduction

Ventilation of the outdoor environment around buildings is necessary for the thermal comfort and environmental health of the inhabitants in and around the buildings. Literatures have shown that the spacing distance between adjacent buildings can significantly influence the outdoor ventilation around the buildings. Ventilation has also been found to generally increase as the spacing distance between buildings increases. However, because of limitations to land availability there is the need to explore intermediate spacing distances which may engender acceptable ventilation around the buildings. Most of existing research studies on wind flow characteristics around arrays of buildings with effect to ventilation focused on those buildings with even street canyons. The few studies on configurations with uneven canyons mainly adopted highly simplified models and are not with reference to actual wind data of an urban area. The present study is aimed at understanding the impacts of the variation of building height and spacing distance on the wind flow and air ventilation around different configurations of a typical two-building layout of the step-up configuration with a taller downwind building. It forms part of the preliminary studies of the broad investigation into the blockage effects of tall buildings to wind flow on arrays of low-rise buildings, aimed at formulating appropriate guidelines for building layout, with consideration for the climatic characteristics of an urban area.

Case Study and Mathematical Formulation

The study uses two blocks of the basic configuration of residential buildings – a single-loaded closed corridor apartment building – to represent the two adjacent buildings. A typical low-wind suburban area for which outdoor air ventilation is most desirable was considered. For this purpose,

a ten-year wind data (2003-2012) obtained from the Malaysia (Subang) Meteorological Data was obtained and used to develop a wind profile for the area. Wind flow in an urban area is commonly in the turbulent flow regime. This was confirmed by the Critical Reynolds number determined to be below 4000 [1]. The isothermal flow is therefore described by the equations of continuity and Navier-Stokes momentum equations. The solution procedure adopted was based on the Reynolds Averaged Navier-Stokes (RANS) approach, with closure for the model equations obtained by the realizable *k-ε* (RKE) turbulence model. The resulting equations are expressed as follows:

$$\frac{\partial \bar{U}_i}{\partial x_i} = 0. \quad (1)$$

$$\bar{U}_j \frac{\partial \bar{U}_i}{\partial x_j} = -\frac{1}{\rho}\frac{\partial \bar{P}}{\partial x_i} + \frac{\partial}{\partial x_j}\left(\nu \frac{\partial \bar{U}_i}{\partial x_j} - \overline{u_i'' u_j''}\right). \quad (2)$$

$$\bar{U}_i \frac{\partial k}{\partial x_i} = \frac{1}{\rho}\frac{\partial}{\partial x_i}\left\{\left(\mu + \frac{\mu_t}{\sigma_k}\right)\right\}\frac{\partial k}{\partial x_i} + \frac{1}{\rho}P_k - \varepsilon. \quad (3)$$

$$\bar{U}_i \frac{\partial \varepsilon}{\partial x_i} = \frac{1}{\rho}\frac{\partial}{\partial x_i}\left\{\left(\mu + \frac{\mu_t}{\sigma_\varepsilon}\right)\right\}\frac{\partial \varepsilon}{\partial x_i} + C_1 S\varepsilon - C_2 \frac{\varepsilon^2}{k+\sqrt{\nu\varepsilon}}. \quad (4)$$

where, $\overline{u_i'' u_j''} = \frac{2}{3}k\delta_{ij} - \nu_t\left(\frac{\partial \bar{U}_i}{\partial x_j} + \frac{\partial \bar{U}_j}{\partial x_i}\right)$; $P_k = \nu_t\left(\frac{\partial \bar{U}_i}{\partial x_j} + \frac{\partial \bar{U}_j}{\partial x_i}\right)\frac{\partial \bar{U}_i}{\partial x_j}$; $\nu_t = \frac{\mu_t}{\rho}$; $\mu_t = \rho C_\mu \frac{k^2}{\varepsilon}$; $C_\mu = \frac{1}{A_0 + A_s\frac{kU^*}{\varepsilon}}$; $A_0 = 4.04$; $A_s = \sqrt{6}\cos\phi$; $\phi = \frac{1}{3}cos^{-1}\left(\sqrt{6}\,W\right)$; $W = \frac{S_{ij}S_{jk}S_{ki}}{\tilde{S}^3}$; $S_{ij} = \frac{1}{2}\left\{\frac{\partial \bar{U}_j}{\partial x_i} + \frac{\partial \bar{U}_i}{\partial x_j}\right\}$; $U^* = \tilde{S} = \sqrt{S_{ij}S_{ij}}$; $C_1 = max\left[0.43, \frac{\eta}{\eta+5}\right]$; $\eta = S\frac{k}{\varepsilon}$; $S = \sqrt{2S_{ij}S_{ij}}$.

$C_{1\varepsilon}$, C_2, σ_k, and σ_ε are model constants and have values as follows: $C_{1\varepsilon} = 1.44$, $C_2 = 1.9$, $\sigma_k = 1.0$, $\sigma_\varepsilon = 1.2$.

The model equations were computed using the commercial CFD codes ANSYS Fluent 14.0 [2].

Validation of the CFD Model

The performance of the CFD model was assessed by comparing the simulation results of the model equations with experimental data from the wind tunnel experiment conducted by a working group of the Architectural Institute of Japan (AIJ) on the flow field around the model of a single high-rise building, aimed at formulating guidelines for the CFD prediction of the pedestrian wind environment around buildings [3]. The geometry of the building model is as shown in Fig.1 below. The computational domain was designed following recommendations of major CFD guidelines [4-7], with the inflow boundary, the lateral and top boundaries set 5h away from the building, while the outflow boundary was located 15h behind the building. 'h' is the height of the model building.

The results of the validation of the CDF turbulence model are as presented in Figs.2 & 3 below. Fig.2 compares the simulation results of the mean streamwise wind velocity component at four locations on a vertical plane along the centreline of the building with the wind tunnel experimental data, while Fig.3 compares the same velocity component at similar locations on a horizontal plane at y = 0.0125m (near the ground surface), for half domain. The mean streamwise wind velocity on the vertical plane along the centreline of the building and the horizontal plane ay y=0.0125 m agreed very well with the experimental data at the measuring points in front of and behind the building.

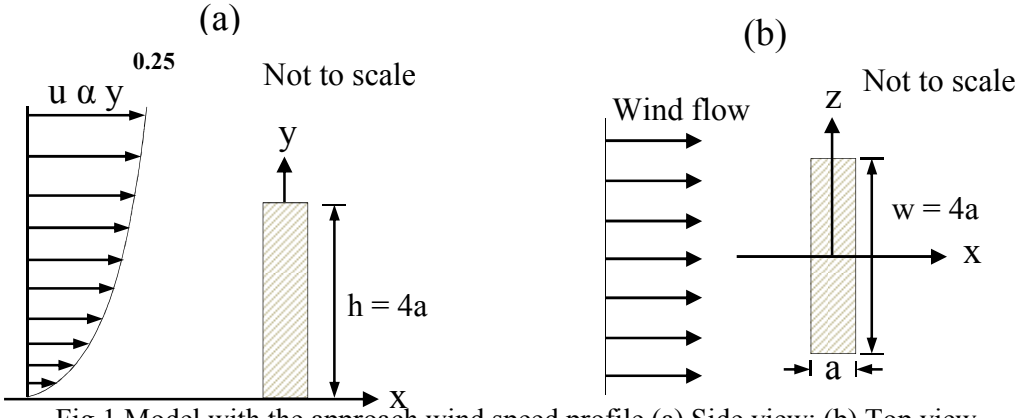

Fig.1 Model with the approach wind speed profile (a) Side view; (b) Top view

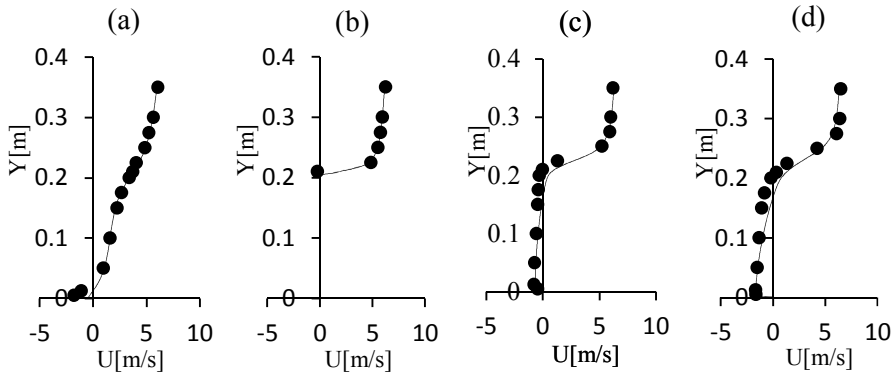

Fig.2 Comparison of wind tunnel experimental data (dotted points) and RKE turbulence model results (solid lines) of mean streamwise wind velocity component u at (a) x = -0.075m; (b) x = 0; (c) x = 0.05m; (d) x = 0.1m on a vertical plane along the centreline of the building.

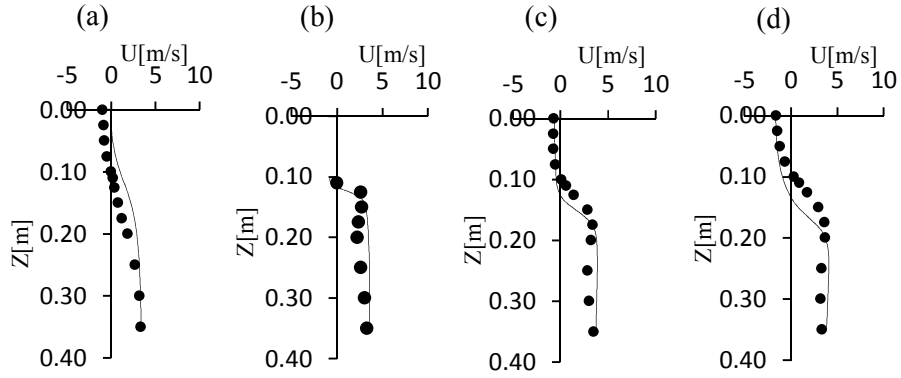

Fig.3 Comparison of wind tunnel experimental data (dotted points) and RKE turbulence model results (solid lines) of mean streamwise wind velocity component u at (a) x = -0.075m; (b) x = 0; (c) x = 0.05m; (d) x = 0.1m on a horizontal plane at y = 0.0125m ($\frac{1}{16}h$), for half domain.

Main Simulation

The two-building configuration simulated consisted of a four-storey building A with a constant height of 12 m and a second building, B, located downwind. The height of B is varied to assess the impact of height of the building on wind flow at the pedestrian level of the street. The different heights of building B considered are 0H (used as reference case, when there is no high-rise building in the neighbourhood of building A), H, 1.5H, 2H, 2.5H, and 3H. The separation distance between the buildings is also varied from 0.5H to 3H with step increment of 0.5H. The configuration and geometry of the two-building structure are as shown in Figs.4 and 5 below. The computational domain was designed following similar procedure as for the validation model. However, the reference height used was the height of the taller building.

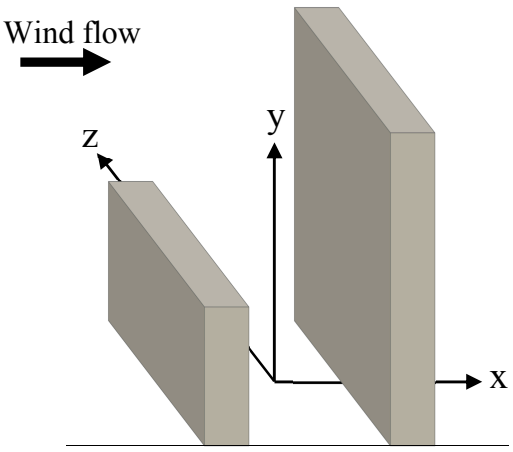

Fig.4 Configuration of the two adjacent buildings

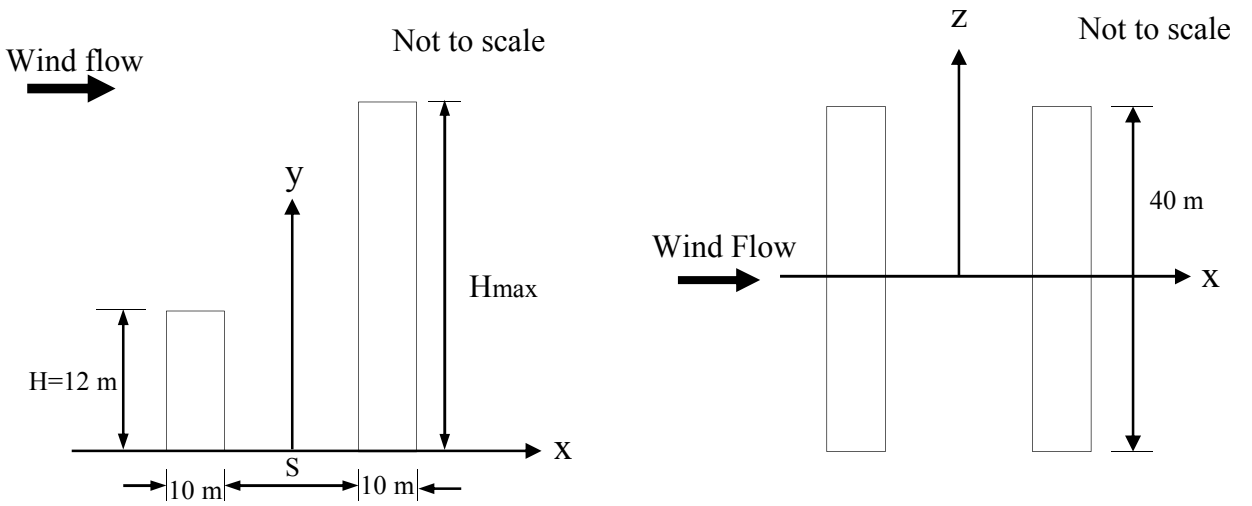

Fig.5 Geometry of the two adjacent buildings showing (a) side view; (b) top view

Performance Criteria for Air Ventilation

The performance of the various configurations of the buildings layout was assessed by two air ventilation indicators called velocity ratio (VR) and air exchange rate (AER). The wind velocity ratio is a dimensionless quantity that compares the velocity at the pedestrian level (2 m above ground surface) with some reference velocity. It is defined according to according to [8-9] as

$$VR = V_p/V_\infty. \tag{5}$$

Here, the reference velocity, V_∞, is taken as the wind velocity at the gradient height.

The air exchange rate denotes the volumetric air exchange per unit time [10,11]. For the present study, the air exchange is across the external boundaries of the cavity bounded by the leeward and windward walls of the two buildings, two x-y planes coplanar with the sides of the buildings, and a horizontal plane on top of the low-rise building. Following [12], for the 3-D system, the temporal positive AER ($\overline{AER+}$) for the air entering into the canyon across the boundaries can be expressed as

$$\overline{AER+} = \sum_{i=1}^{2} \int_\Gamma \overline{W_+} d\Gamma\Big|_{side\ i} + \int_\Gamma \overline{V_+} d\Gamma\Big|_{Top} + \sum_{i=1}^{3} \frac{1}{\sqrt{6}} \int_\Gamma \sqrt{k}\, d\Gamma\Big|_{plane\ i}. \tag{6}$$

where, $\overline{W_+}$ and $\overline{V_+}$ are the mean positive transverse and vertical velocity components, w_+'' and v_+'' are the mean positive transverse velocity and vertical velocity fluctuations, and k the turbulent kinetic energy on the ventilation boundaries Γ.

Results and Discussion

The results of the air ventilation characteristics of the various configurations of the layout of the two adjacent buildings are as presented in Figs.6-9. Fig.6 shows the variation of velocity ratio with height ratio, while Fig.8 is the variation of dimensionless air exchange rate with height ratio. Figs.7 & 9 are respectively the extended views of Figs.6 & 8, to include velocity ratio data at HR 0. The HR 0 indicated in the figures is for the reference case when there is no building adjacent to the low-rise building.

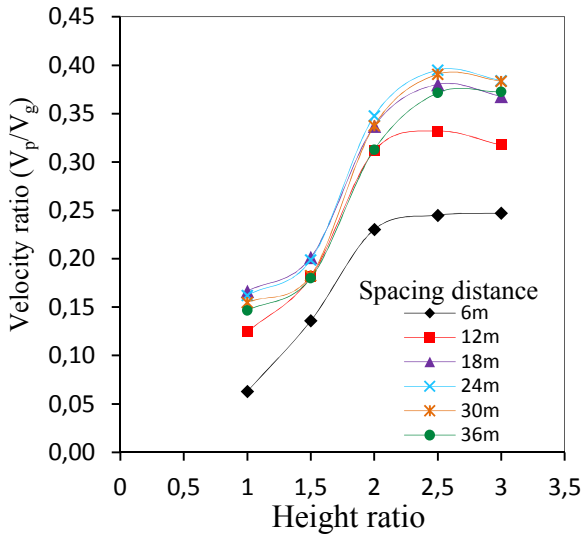

Fig.6 Variation of velocity ratio with height ratio for different spacing distances

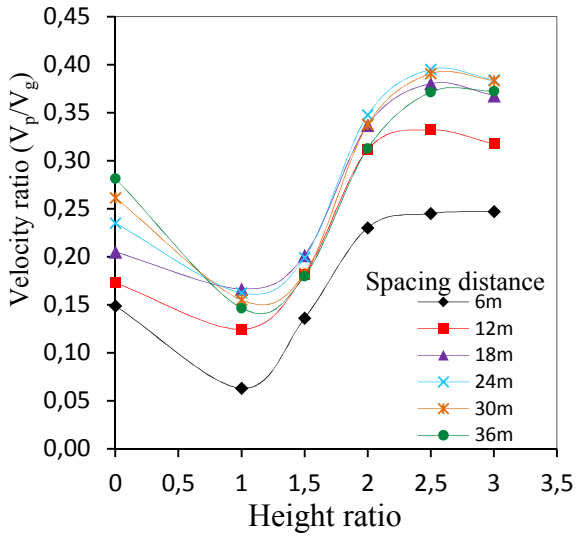

Fig.7 Extended view of Fig.6 including velocity ratio data at HR 0

From Fig.6 it would be observed that velocity ratio generally increases with height ratio from HR1.0 to HR 2.5. However, there is a critical jump of VR from HR 1.5 to HR 2.0. It would also be observed that velocity ratio increases with spacing distance up to a certain maximum for each height ratio before falling off to lower values with further increase in spacing distance. This indicates that more air motion is induced at the pedestrian level as the height of the downwind building increases. This is in contrast to such building arrangement in which the upwind building has a greater height. In this step-up configuration, this may be due to the increased windward surface area of the downwind building channelling greater quantity of air down to the pedestrian level from the stagnation zone on the surface. For each of the height ratios, there is a spacing distance at which the velocity ratio is highest. For HRs 1.0 and 1.5, this maximum occurs at 18 m spacing distance, while for HRs 2.0 to 3.0 the maximum values occur at S 24 m. From Fig.7, it would be seen that the maximum velocity ratio does not necessarily occur at HR 0; rather it occurs at HRs > 1.5 for each of the spacing distances. This implies that air motion greater than obtainable for an isolated low-rise building could be induced when the building is adjacent to a downwind building with greater height ratios. This result is consistent with those reported in previous studies [13-15].

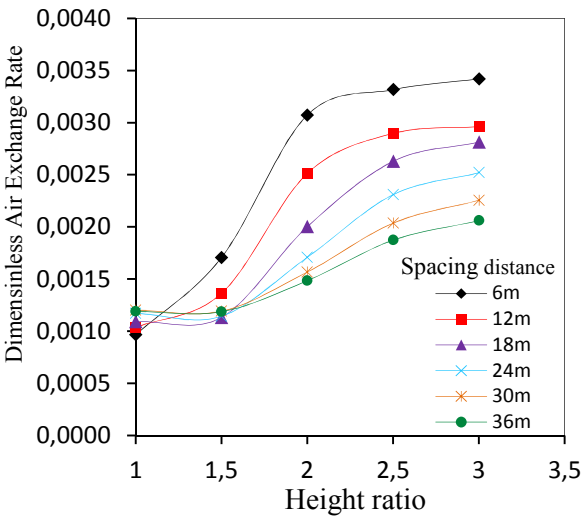

Fig.8 Dimensionless air exchange rate against height ratio for various spacing distances

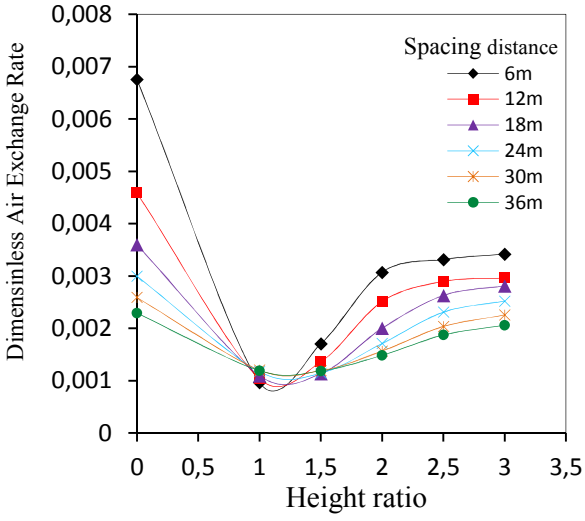

Fig.9 Extended view of Fig.8 including velocity ratio data at HR 0

Fig.8 shows that dimensionless air exchange rate generally increases with height ratio, while it decreases with spacing distance except for HR 1.0 and 1.5. The first part of this result indicates that greater quantity of air from within the cavity between the buildings is exchanged with air from outside the cavity, which should result in better air quality. The result is consistent with that obtained for velocity ratio in Fig.6. For HR 0 the exchange rate increases with spacing distance, while for HR 1.5 it initially decreases with spacing distance before increasing mildly with the spacing distance. From Fig.9 it would be observed that the exchange rate for the reference case HR 0 is greatest for each of the spacing distances.

Conclusion

The air ventilation characteristics of various step-up configurations of a layout of two adjacent buildings have been investigated in this research work. Three-dimensional simulation of the flow by which effects of turbulent flow features could be captured and which utilize representative building geometry and actual wind data was conducted. The critical parameters studied are the separation distance between the buildings and buildings height ratio, and the air ventilation performance criteria adopted are wind velocity ratio and air exchange rate. It was shown that velocity ratio generally increases with height ratio. This indicates that more air motion is induced at the pedestrian level as the height of the downwind building increases. For each of the height ratios, there is a spacing distance at which the velocity ratio is highest. For HRs 1.0 and 1.5, this maximum occurs at 18 m spacing distance, while for HRs 2.0 to 3.0 the maximum values occur at S 24 m. Configurations with HRs > 1.5 induces greater air motion at the pedestrian level than the case of isolated building. The dimensionless air exchange rate generally increases with height ratio, indicating that greater quantity of air from within the cavity between the buildings is exchanged with air from outside the cavity, which should result in better air quality. The findings of the study demonstrate the importance of incorporating wind data of an urban area in formulating guidelines for layout of buildings.

Acknowledgement

The authors would like to thank the CICT Unit of Universiti Teknologi Malaysia (UTM) for providing the computational support for conducting the research.

References

[1] K. Uehara, S. Murakami, S. Oikawa, S. Wakamatsu, Wind tunnel experiments on how thermal stratification affects flow in and above urban street canyons, Atmospheric Environment. 34 (2000) 1553-1562.

[2] Ansys (2011). ANSYS Release 14.0. User's Guide, Canonsburg, ANSYS Inc.

[3] Y. Tominaga, A. Mochida, T. Shirasawa, R. Yoshie, H. Kataoka, K. Harimoto, T. Nozu, Cross comparisons of CFD results of wind environment at pedestrian level around a high-rise building and within a building complex, Journal of Asian architecture and building engineering. 3 (2004) 63-70.

[4] Y. Tominaga, A. Mochida, R. Yoshie, H. Kataoka, T. Nozu, M. Yoshikawa, T. Shirasawa, AIJ guidelines for practical applications of CFD to pedestrian wind environment around buildings, Journal of Wind Engineering and Industrial Aerodynamics. 96 (2008) 1749-1761.

[5] E. Ng, L. Katzschner, U. Wang, C. Ren, L. Chen, Working Paper No. 1A: draft urban climatic analysis map–urban climatic map and standards for wind environment–feasibility study, Technical Report for Planning Department HKSAR, Report No. WP1A, Planning Department of Hong Kong Government: Hong Kong, (2008).

[6] J. Franke, Recommendations of the COST action C14 on the use of CFD in predicting pedestrian wind environment, in: The fourth international symposium on computational wind engineering, Yokohama, Japan, 2006, 529-532.

[7] J. Franke, A. Hellsten, K.H. Schlunzen, B. Carissimo, (Eds.), Best practice guideline for the CFD simulation of flows in the urban environment, COST Action 732, quality assurance and improvement of microscale meteorological models, Brussels, COST office, (2007).

[8] J. Franke, C. Hirsch, A.G. Jensen, H.W. KruS, M. Schatzmann, P.S. Westbury, S.D. Miles, J.A. Wisse, N.G. Wright, Recommendations on the use of CFD in wind engineering, in: Proceedings of the International Conference on Urban Wind Engineering and Building Aerodynamics, in: van Beeck, J.P.A.J.(Ed.), COST Action C14, Impact of Wind and Storm on City Life Built Environment, 5–7 May 2004 von Karman Institute, Sint-Genesius-Rode, Belgium.

[9] S.H.L. Yim, J.C.H. Fung, A.K.H. Lau, S.C. Kot, Air ventilation impacts of the "wall effect" resulting from the alignment of high-rise buildings. Atmospheric Environment. 43 (2009) 4982-4994.

[10] X-X. Li, C-H. Liu, D.Y.C. Leung, Development of a k-ϵ model for the determination of air exchange rates for street canyons, Atmospheric Environment. 39 (2005) 7285-7296.

[11] C-H. Liu, D.Y. Leung, M.C. Barth, On the prediction of air and pollutant exchange rates in street canyons of different aspect ratios using large-eddy simulation, Atmospheric Environment. 39 (2005) 1567-1574.

[12] X. Xie, C-H. Liu, D.Y. Leung, M.K. Leung, Characteristics of air exchange in a street canyon with ground heating. Atmospheric Environment. 40 (2006) 6396-6409.

[13] X. Xie, Z. Huang, J-S. Wang, Impact of building configuration on air quality in street canyon, Atmospheric Environment. 39 (2005) 4519-4530.

[14] J-S. Wang, Z. Huang, Numerical study on flow and dispersion in rban street canyons of asymmetrical configurations, Journal of Hydrodynamics, Ser. B. 18 (2006) 146-150.

[15] J-S. Wang, B-Q. Zhao, C. Ye, D-Q. Yang, Z. Huang, Optimizing layout of urban street canyon using numerical simulation coupling with mathematical optimization, Journal of Hydrodynamics, Ser. B. 18 (2006) 345-351.